

# Electrical conductivity in oxygen-substituted $\text{SrTiO}_{3-\delta}$ films

M. Tyunina,<sup>1,2\*</sup> M. Savinov,<sup>2</sup> A. Dejneka<sup>2</sup>

<sup>1</sup>Microelectronics Research Unit, Faculty of Information Technology and Electrical Engineering, University of Oulu, P. O. Box 4500, FI-90014 Oulu, Finland

<sup>2</sup>Institute of Physics of the Czech Academy of Sciences, Na Slovance 2, 18221 Prague, Czech Republic

Enhancement of electrical conductivity in fundamentally insulating  $\text{ABO}_3$  perovskite oxide ferroelectrics is crucial for innovative applications in resistive switching, photovoltaics, and catalysis. One of the methods to raise conductivity in bulk crystals or ceramics relies on the possibility to remove and/or substitute oxygen atoms. Here, we explored this approach for thin films of the representative perovskite oxide  $\text{SrTiO}_3$ . Small-signal AC conductivity was investigated in epitaxial and polycrystalline films, where oxygen vacancies ( $\text{V}_\text{O}$ ), nitrogen (N), or hydrogen (H) were introduced *in-situ* during film growth. Hopping mechanism of conductivity was evidenced by the observed strong growth of AC conductivity with temperature, frequency, and AC voltage in all films. Small polarons were identified as charge carriers. Oxygen vacancies/substitutions were suggested to facilitate hopping probability by generating sites for carrier localization. Important ferroelectric devices were proposed to benefit from the revealed hopping conductivity owing to its unique increase with electric field.

\*Corresponding author: [marina.tjunina@oulu.fi](mailto:marina.tjunina@oulu.fi)

Electrical conductivity is critical for nearly all applications of multifunctional  $ABO_3$ -type perovskite oxide ferroelectrics. Mainstream applications (e.g., in capacitors, electromechanical, and electrooptical devices) demand perfect insulating properties, which are ensured by a fundamental wide-bandgap insulator state in ferroelectrics. On contrary, innovative applications in resistive switching, photovoltaics, and catalysis ask for semiconductor- or metal-like behaviour with relatively large conductivity. Such conductivity can be achieved using appropriate cationic doping. Additionally, increased conductivity is often obtained as a result of high-temperature processing, which is performed at low pressures of oxygen, in vacuum, or in the presence of hydrogen or nitrogen, and lasts from a few hours to several days. For instance, in one of the best studied representatives of a broad class of ferroelectrics, strontium titanate ( $SrTiO_3$ , STO), this approach has been employed for over a half century and includes recent developments in topochemical synthesis.<sup>1-15</sup> Because oxygen atoms are removed and/or replaced during this high-temperature processing, it is referred to as “reduction” and the increased conductivity is commonly related to the presence of oxygen vacancies/substitutions. Today, this phenomenon attracts particular interest because of its essential role in thin-film memristive devices.<sup>16-18</sup> Notably, it was found that apart from oxygen vacancies/substitutions, also other point or extended defects<sup>19-26</sup> as well as surface two-dimensional electron gas (2DEG)<sup>27-38</sup> can raise the electrical conductivity in STO films.

In this work, we aimed to employ oxygen vacancies/substitutions for controlling the electrical conductivity of thin STO films. We investigated the conductivity in epitaxial and polycrystalline films, where oxygen vacancies, nitrogen substitutions, or hydrogen substitutions were introduced *in-situ* during film growth.<sup>39-40</sup> To diminish possible impact of surface 2DEG, we determined the conductivity in the films sandwiched between the bottom and top electrodes in the vertical structures. To avoid injection of excess carriers and inspect intrinsic conductivity, we applied small-signal AC impedance spectroscopy.<sup>41</sup> Furthermore, to distinguish between the band and hopping mechanisms of conductivity, we analyzed the conductivity as a function of the temperature, frequency, and amplitude of AC voltage.<sup>42-51</sup>

Our studies revealed insulator-type hopping conductivity with small polarons as charge carriers. These observations suggest that oxygen vacancies/substitutions yield sites for electronic localization and hopping. Fundamentally, the hopping conductivity is strongly dependent on the electric field and relevant for all perovskite-type oxide ferroelectrics. Therefore, the hopping

conductivity may have essential implications for all ferroelectric devices including vital resistive switching diodes.

We investigated the conductivity in thin (80-100 nm) epitaxial and polycrystalline STO films, which were grown in pairs within a single pulsed laser deposition process, thus ensuring similar chemical composition for both films in each pair.<sup>39</sup> Epitaxial films were prepared on (001)  $(\text{La}_{0.3}\text{Sr}_{0.7})(\text{Al}_{0.65}\text{Ta}_{0.35})\text{O}_3$  substrates using epitaxial  $\text{LaNiO}_3$  bottom electrodes, whereas polycrystalline films were formed on Pt-coated Si substrates. Oxygen substitution was implemented by varying the gas ambience during deposition.<sup>39-40</sup> For brevity, we denote stoichiometric, oxygen-deficient, nitrogen-doped, and hydrogen-doped films by S, O, N, and H, correspondingly, for epitaxial films, and by S\*, O\*, N\*, and H\* for polycrystalline films. The content  $\delta$  was from 0 to  $\sim 0.3$  in  $\text{SrTiO}_{3-\delta}\text{X}_\delta$  [Supplementary section S1]. We note that in addition to compositional analyses, elastic interactions of defects with substrate-induced misfit strain make it possible to estimate defect concentration from the lattice parameters in epitaxial films.<sup>40</sup> The STO/LSAT films were (001)-oriented, whereas the STO/Si films were randomly-oriented [Supplementary section S2].

For electrical characterization, Pt top electrodes were formed by pulsed laser deposition using a shadow mask. The impedance was measured on a NOVOCONTROL Alpha-AN High Performance Frequency Analyzer, and the control of temperature was realized using Linkam cold/hot stages. The conductivity of the bottom electrodes was also examined.

To identify the mechanism of conductivity, the AC conductivity was investigated as a function of temperature  $T = 80 - 500$  K, frequency  $f = 1 - 10^6$  Hz, and amplitude of the AC probing signal  $V_{AC} = 10^{-3} - 1$  V. This approach is justified in Supplementary section S3. The key characteristic features of the hopping conductivity compared to those of the band conductivity are adopted from Refs. 42-51 and summarized in Table I.

**Table I.** Simplified approximations for changes in the band conductivity and hopping conductivity with temperature, frequency, and voltage.

factors	BAND conductivity	HOPPING conductivity
temperature $T$	$\exp(-T^{-1})$	$\exp(-T^{-b}), b \leq 1$
frequency $f$	$\text{const}(f)$	$f^s, s \leq 2$
small voltage $V$	$\text{const}(V)$	$\exp(-V^{-1})$
large voltage $V$	$\exp(V^{-1})$	$\exp(-V^{-1})$

injection ( $V, T$ )		
SCL	$V$	
FN	$V \exp(-V^{-1})$	
RS	$T^2 \exp(\sqrt{V})$	

(SCL – space charge limited, FN - Fowler-Nordheim, and RS - Richardson-Schottky mechanisms)

The measured AC conductivity is presented as a function of frequency  $f$ , temperature,  $T$ , and voltage  $V_{AC}$  in Figs. 1-2 and Supplementary Figs. S2-S8. All films exhibit a very small conductivity of  $\sim 10^{-13}$ - $10^{-11}$  S/cm at low  $T, f$ , and  $V_{AC}$  [e.g., see data for  $T = 100$  K and  $f = 1$  Hz in Fig. 1]: values that imply excellent insulating properties. The insulating properties are consistent with the optical observations, which evidenced the wide bandgaps and absence of free carriers in such films.<sup>39-40</sup>

Importantly, the conductivity strongly increases with increasing frequency [Fig. 1 and Supplementary Figs. S2-S3]. Moreover, the conductivity increase for frequencies from 1 Hz to 1 MHz is comparable to or even larger than that for temperatures from 100 K to 500 K. Such a massive frequency dispersion firmly evidences the hopping mechanism of charge transport.

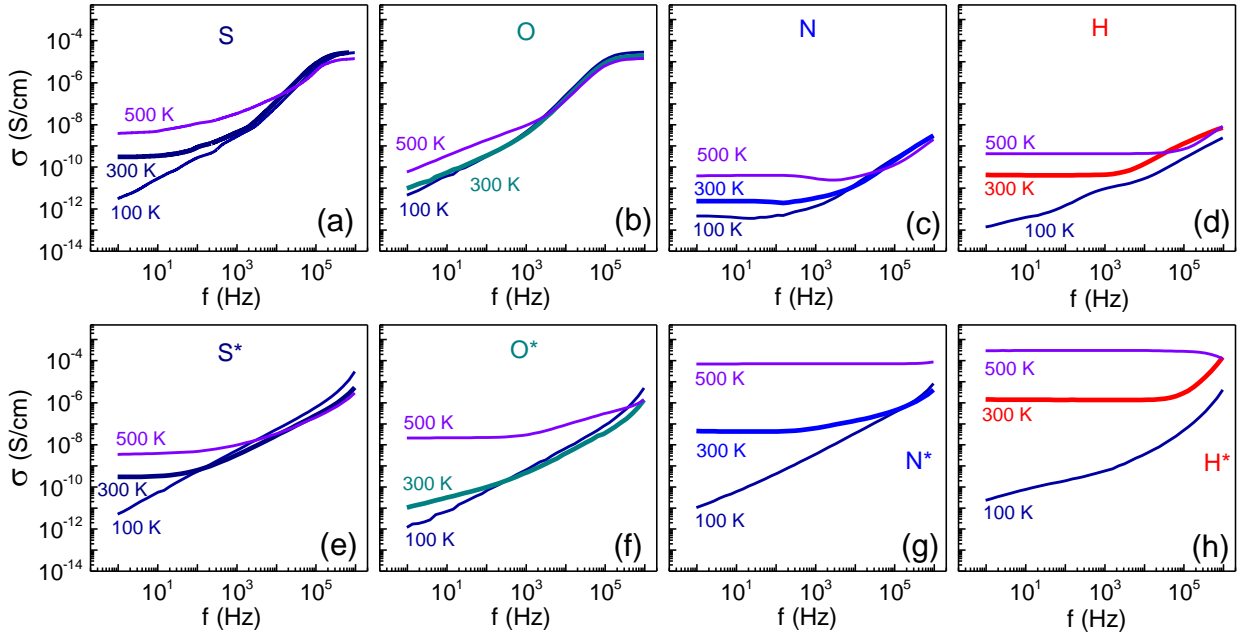


**Fig. 1.** Log-log plots of conductivity (at  $V_{AC} = 1$  mV) as a function of frequency at temperatures of 100, 300, and 500 K (as marked on the plots) in the (a-d) epitaxial and (e-h) polycrystalline films.

The film-specific strong frequency dispersion and temperature dependence of the conductivity make it difficult to directly compare the anion-substituted and stoichiometric films. However, the obtained results imply two opposite tendencies, which are produced by anion substitution: the conductivity tends to decrease in the epitaxial films [Figs. 1(a-d) and Supplementary Figs. S2(a, b)] and it tends to increase in the polycrystalline films [Figs. 1(e-h) and Supplementary Figs. S2(c, d)]. The seemingly counterintuitive behaviour of the epitaxial films suggests a reduced concentration of sites for hopping in the doped films, that, however, is fully consistent with the improved crystal quality (less structural defects) of such films.<sup>39-40</sup> Notably, for temperatures higher than 200 K, the conductivity in the doped polycrystalline films is up to several orders of magnitude larger than that in the epitaxial films [Supplementary Fig. S3]. This huge difference lends additional proof towards the hopping transport. Compared to the single-crystal epitaxial films, the polycrystalline films are enriched with deviations from a perfect monocrystalline structure. These defects enable a high density of available sites for localization and hopping of charge carriers. The high density, broad distribution of energies, and spatial proximity of these sites ensure increased hopping probability and, hence, an enlarged conductivity in the polycrystalline films.<sup>44</sup>

The hopping mechanism is further confirmed by the specific dependence of the conductivity on the amplitude  $V_{AC}$  of the AC voltage. In all films, the conductivity increases with  $V_{AC}$ , whereas the increase is better expressed in the polycrystalline films [Fig. 2 and Supplementary Fig. S4].

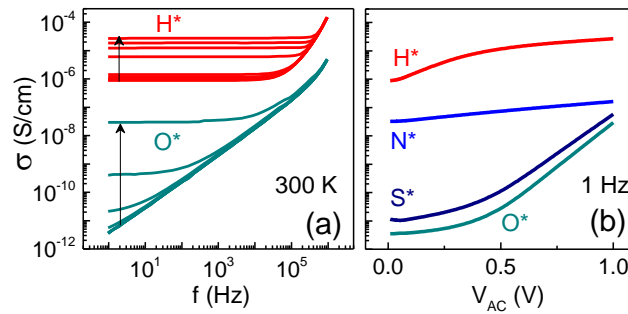


**Fig. 2.** (a) Log-log plots of the room-temperature conductivity as a function of frequency at different AC voltages and (b) semilog plots of the room-temperature conductivity as a function of AC voltage at  $f = 1$  Hz in the polycrystalline films. Arrows show directions of the voltage increase in (a).

The profound concurrent impacts of the temperature, frequency, and voltage on the conductivity [see also Supplementary Fig. S5 for illustration] are fully consistent with the hopping transport. It is worth mentioning that the observed variations in the conductivity with  $T$ ,  $f$ , and/or  $V_{AC}$  well exceed those, which are induced by anion modifications as such.

Various charge carriers (electrons, holes, small polarons, and/or coupled polarons) and hopping processes (tunneling, barrier, adiabatic, variable-range, *etc*) may be involved in charge transport. To gain insight into the type of charge carriers, we first analyzed low-frequency conductivity ( $f = 1$  Hz) as a function of temperature. Good fits to  $[\sigma \propto \exp(-1/T)]$  are obtained above room temperature in all films [Supplementary Fig. S6]. At low temperatures, the curves  $[\ln(\sigma)$  vs  $1/T]$  flatten. The observed shape of the temperature dependence of conductivity is typical for hopping of small polarons.<sup>45</sup> The hopping barriers, extracted from the linear fits, are in the range of 0.1 – 0.3 eV in the epitaxial films and 0.3 – 0.5 eV in the polycrystalline films, and are also consistent with the binding energies of small polarons.<sup>45</sup>

Next, we more closely inspected the substantial frequency dispersion of the conductivity [Figs. 1(a-f)]. The plots of  $[\ln(\sigma)$  versus  $\ln(f)]$  for different fixed temperatures [Supplementary Fig. S7 and Fig. S8] contain linear fractions, implying power-law relationships  $[\sigma \propto f^s]$ . The exponents  $s$ , determined from the linear fits  $[\ln(\sigma) \propto \ln(f)]$ , are displayed as a function of temperature in Fig. 3.

The dielectric permittivity is frequency-independent [Supplementary Fig. S9], implying that the behaviour of  $s$  is not related to dielectric relaxation. Concurrently, the frequency-independent dielectric loss gives a contribution with the temperature-independent  $s = 1$ , which is not the case in Fig. 3. In the epitaxial films, two distinct relaxation processes coexist. The higher-frequency relaxation is characterized by  $s > 1$ , which is practically temperature independent. Although comprehensive theoretical analysis of such behavior is still required, a phononless or a nearly constant loss tunneling may be responsible for it.<sup>44</sup> Quantum mechanical tunneling of small polarons can also lead to a temperature-independent  $s \leq 1$ , whereas a barrier hopping gives  $s \leq 1$ , which decreases on heating.<sup>44,45,47,51</sup> Compared to the tunnelling processes and barrier hopping of small polarons in the epitaxial films, dominant barrier hopping is likely in the polycrystalline films.

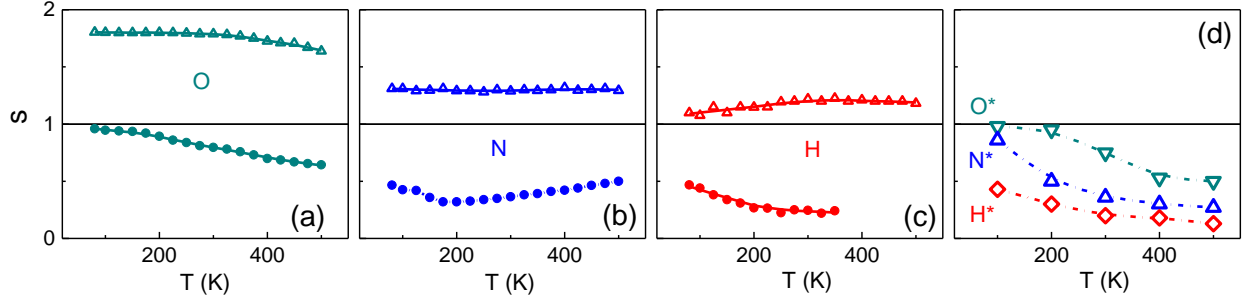


**Fig. 3.** Relaxation exponents  $s$  as a function of temperature in the (a-c) epitaxial and (d) polycrystalline films.

The presented experimental observations signify hopping of small polarons in the oxygen-substituted STO films. We note that despite clear optical evidence of small polarons in STO (see Ref. 52 and references therein), their hopping transport is not sufficiently recognized. In STO, the small polarons are intrinsic and/or injected electrons, which are localized, or trapped, on the  $\text{Ti}^{4+}$  sites, thus turning them into  $\text{Ti}^{3+}$  sites.<sup>52,53</sup> Both self-trapping and trapping, assisted by extended and/or point defects, can occur and lead to a rich landscape of hopping sites in terms of their energies and coordinates.<sup>54</sup> In this picture, oxygen vacancies/substitutions facilitate conductivity by yielding hopping sites and thus raising the hopping probability. Concurrently, not only oxygen vacancies/substitutions may be responsible for the presence of  $\text{Ti}^{3+}$  and the conductivity increase. We also note that the trapping and hopping of carriers do not exclude trap-to-band transitions and band conductivity under sufficient thermal, electrical, or photostimulated excitation. Likewise, the band and hopping mechanisms can coexist in cation-modified STO.

Fundamentally, carrier localization is characteristic not specifically for STO but for all perovskite-type oxide ferroelectrics.<sup>45</sup> Thus, hopping conductivity is relevant for these materials in general. An important feature of the hopping conductivity is its massive growth with an electric field  $E$  [ $\sigma \propto \exp(-1/E)$ ],<sup>44</sup> which can enable an orders-of-magnitude rise in current with a DC bias in thin films. Such a rise contrasts with the saturation of current at high fields for the band conductivity and is not limited by the injection current. Accordingly, hopping conductivity may empower innovative ferroelectric devices, including advanced resistive switching diodes, and is worthy of more research attention.

In summary, the electrical AC conductivity was investigated in a broad range of temperatures from 80 to 500 K, frequencies from 1 Hz to 1 MHz, and AC voltages from 1 meV to 1 V in thin

*in-situ* oxygen-substituted epitaxial and polycrystalline  $\text{SrTiO}_{3-\delta}\text{X}_\delta$  ( $\text{X} = \text{V}_\text{O}$ , N, or H) films sandwiched between the bottom and top electrodes. The conductivity was found to strongly increase with temperature, frequency, and AC voltage. The observations evidenced the hopping mechanism of charge transport. The analysis revealed small polarons as charge carriers. It was suggested that oxygen vacancies/substitutions, in resemblance and combination with other defects, produce sites for carrier localization and hopping, thus raising the hopping probability and conductivity. It was also proposed that profound electric field dependence of hopping conductivity may be beneficial for innovative ferroelectric devices.

See the supplementary material for (I) anionic content, (II) crystal orientation, (III) basic features of conductivity, and (IV) analyses of temperature dependence and frequency dispersion.

The authors would like to thank T. Kocourek, O. Pacherova, S. Cichon, and P. Babor for sample preparation and characterization. The authors acknowledge support from the Czech Science Foundation (Grant No. 19-09671S) and the European Structural and Investment Funds and the Ministry of Education, Youth and Sports of the Czech Republic through Programme “Research, Development and Education” (Project No. SOLID21 - CZ.02.1.01/0.0/0.0/16\_019/0000760).

## DATA AVAILABILITY

The data that support the findings of this study are available within the article and its supplementary material.

## REFERENCES

- <sup>1</sup> H. P. R. Frederikse, W. R. Thurber, W. R. Hosler, *Phys. Rev.* **134**, A442 (1964).
- <sup>2</sup> O. N. Tufte, P. W. Chapman, *Phys. Rev.* **155**, 796 (1967).
- <sup>3</sup> J. E. Carnes and A. M. Goodman, *J. Appl. Phys.* **38**, 3091 (1967).
- <sup>4</sup> D. Parker and J. Yahia, *Phys. Rev.* **169**, 605 (1968).
- <sup>5</sup> C. Lee, J. Yahia, and J. L. Brebner, *Phys. Rev. B* **3**, 2525 (1971).
- <sup>6</sup> C. Lee, J. Destry, J. L. Brebner, *Phys. Rev. B* **11**, 2299 (1975).
- <sup>7</sup> D. A. Crandles, B. Nicholas, C. Dreher, C. C. Homes, A. W. McConnell, B. P. Clayman, W. H. Gong, and J. E. Greedan, *Phys. Rev. B* **59**, 12842 (1999).



- <sup>8</sup> K. Szot, W. Speier, R. Carius, U. Zastrow, and W. Beyer, *Phys. Rev. Lett.* **88**, 075508 (2002).
- <sup>9</sup> A. Spinelli, M. A. Torija, C. Liu, C. Jan, and C. Leighton, *Phys. Rev. B* **81**, 155110 (2010).
- <sup>10</sup> C. Collignon, X. Lin, C.W. Rischau, B. Fauqué, and K. Behnia, *Annu. Rev. Condens. Matter Phys.* **10**, 25 (2019).
- <sup>11</sup> C. Rodenbücher, C. Guguschev, C. Korte, S. Bette, K. Szot, *Crystals* **11**, 744 (2021).
- <sup>12</sup> Y. Kobayashi, O. J. Hernandez, T. Sakaguchi, T. Yajima, T. Roisnel, Y. Tsujimoto, M. Morita, Y. Noda, Y. Mogami, A. Kitada, M. Ohkura, S. Hosokawa, Z. Li, K. Hayashi, Y. Kusano, J. e. Kim, N. Tsuji, A. Fujiwara, Y. Matsushita, K. Yoshimura, K. Takegoshi, M. Inoue, M. Takano and H. Kageyama, *Nat. Mater.* **11**, 507 (2012).
- <sup>13</sup> T. Yajima, F. Takeiri, K. Aidzu, H. Akamatsu, K. Fujita, W. Yoshimune, M. Ohkura, S. Lei, V. Gopalan, K. Tanaka, C. M. Brown, M. A. Green, T. Yamamoto, Y. Kobayashi and H. Kageyama, *Nat. Chem.* **7**, 1017 (2015).
- <sup>14</sup> T. Yajima, A. Kitada, Y. Kobayashi, T. Sakaguchi, G. Bouilly, S. Kasahara, T. Terashima, M. Takano and H. Kageyama, *J. Am. Chem. Soc.* **134**, 8782 (2012).
- <sup>15</sup> G. Bouilly, T. Yajima, T. Terashima, W. Yoshimune, K. Nakano, C. Tassel, Y. Kususe, K. Fujita, K. Tanaka, T. Yamamoto, Y. Kobayashi and H. Kageyama, *Chem. Mater.* **27**, 6354 (2015).
- <sup>16</sup> R. Waser, R. Dittmann, G. Staikov, K. Szot, *Adv. Mater.* **21**, 2632 (2009).
- <sup>17</sup> T. Heisig, C. Baeumer, U. N. Gries, M. P. Mueller, C. La Torre, M. Luebben, N. Raab, H. Du, S. Menzel, D. N. Mueller, C.-L. Jia, J. Mayer, R. Waser, I. Valov, R. A. De Souza, R. Dittmann, *Adv. Mater.* **30**, 1800957 (2018).
- <sup>18</sup> R. Waser, R. Dittmann, S. Menzel, T. Noll, *Faraday Discuss.* **213**, 11-27 (2019).
- <sup>19</sup> M. Kim, G. Duscher, N. D. Browning, K. Sohlberg, S. T. Pantelides, S. J. Pennycook, *Phys. Rev. Lett.* **86**, 4056 (2001).
- <sup>20</sup> K. Szot, W. Speier, G. Bihlmayer, R. Waser, *Nat. Mater.* **5**, 312 (2006).
- <sup>21</sup> B. Liu, V. R. Cooper, Y. Zhang, W. J. Weber, *Acta Mater.* **90**, 394-399 (2015).
- <sup>22</sup> W. Lee, S. Yoo, K. J. Yoon, I. W. Yeu, H. J. Chang, J.-H. Choi, S. Hoffmann-Eifert, R. Waser, C. S. Hwang, *Sci. Rep.* **6**, 20550 (2016).
- <sup>23</sup> F. V. E. Hensling, H. Du, N. Raab, C.-L. Jia, J. Mayer, R. Dittmann, *APL Mater.* **7**, 101127 (2019).

- <sup>24</sup> C. Rodenbücher, K. Bittkau, G. Bihlmayer, D. Wrana, T. Gensch, C. Korte, F. Krok, K. Szot, *Sci. Rep.* **10**, 17763 (2020).
- <sup>25</sup> A. Baki, J. Stöver, T. Schulz, T. Markurt, H. Amari, C. Richter, J. Martin, K. Irmscher, M. Albrecht, J. Schwarzkopf, *Sci. Rep.* **11**, 7497 (2021).
- <sup>26</sup> J. L. Rieck, F. V. E. Hensling, R. Dittmann, *APL Mater.* **9**, 021110 (2021).
- <sup>27</sup> A. F. Santander-Syro, O. Copie, T. Kondo, F. Fortuna, S. Pailhes, R. Weht, X. G. Qiu, F. Bertran, A. Nicolaou, A. Taleb-Ibrahimi, P. Le Fevre, G. Herranz, M. Bibes, N. Reyren, Y. Apertet, P. Lecoeur, A. Barthelemy, M. J. Rozenberg, *Nature* **469**, 189 (2011).
- <sup>28</sup> W. Meevasana, P. D. C. King, R. H. He, S-K. Mo, M. Hashimoto, A. Tamai, P. Songsiriritthigul, F. Baumberger, Z-X. Shen, *Nat. Mater.* **10**, 114 (2011).
- <sup>29</sup> G. Khalsa, A. H. MacDonald, *Phys. Rev. B* **86**, 125121 (2012).
- <sup>30</sup> Z. Wang, Z. Zhong, X. Hao, S. Gerhold, B. Stöger, M. Schmid, J. Sánchez-Barriga, A. Varykhalov, C. Franchini, K. Held, U. Diebold, *Proc. Natl. Acad. Sci. U.S.A.* **111**, 3933 (2014).
- <sup>31</sup> S. McKeown Walker, F. Y. Bruno, Z. Wang, A. de la Torre, S. Riccò, A. Tamai, T. Kim, M. Hoesch, M. Shi, M. S. Bahramy, P. King, F. Baumberger, *Adv. Mater.* **27**, 3894 (2015).
- <sup>32</sup> P. Delugas, V. Fiorentini, A. Mattoni, A. Filippetti, *Phys. Rev. B* **91**, 115315 (2015).
- <sup>33</sup> S. Gonzalez, C. Mathieu, O. Copie, V. Feyer, C. M. Schneider, N. Barrett, *Appl. Phys. Lett.* **111**, 181601 (2017).
- <sup>34</sup> S. N. Rebec, T. Jia, H. M. Sohail, M. Hashimoto, D. Lu, Z.-X. Shen, R. G. Moore, *Proc. Natl. Acad. Sci. U.S.A.* **116**, 16687 (2019).
- <sup>35</sup> S. Cook, M. T. Dylla, R. A. Rosenberg, Z.R. Mansley, G. J. Snyder, L. D. Marks, D. D. Fong, *Adv. Electron. Mater.* **5**, 1800460 (2019).
- <sup>36</sup> K. Han, K. Hu, X. Li, K. Huang, Z. Huang, S. Zeng, D. Qi, C. Ye, J. Yang, H. Xu, A. Ariando, J. Yi, W. Lü, S. Yan, X. R. Wang, *Sci. Adv.* **5**, 7286 (2019).
- <sup>37</sup> Y. Takeuchi, R. Hobara, R. Akiyama, A. Takayama, S. Ichinokura, R. Yukawa, I. Matsuda, and M. D'Angelo, R. Yukawa, K. Ozawa, S. Yamamoto, T. Hirahara, S. Hasegawa, M. G. Silly, F. Sirotti, and I. Matsuda, *Phys. Rev. Lett.* **108**, 116802 (2012).
- <sup>38</sup> S. Hasegawa, *Phys. Rev. B* **101**, 085422 (2020).
- <sup>39</sup> M. Tyunina, O. Pacherova, N. Nepomniashchaia, V. Vetokhina, S. Cichon, T. Kocourek, A. Dejneka, *Phys. Chem. Chem. Phys.* **22**, 24796 (2020).

- <sup>40</sup> M. Tyunina, L. L. Rusevich, E. A. Kotomin, O. Pacheroova, T. Kocourek and A. Dejneka, J. Mater. Chem. C **9**, 1693 (2021).
- <sup>41</sup> M. Tyunina, M. Savinov, Phys. Rev. B **101**, 094106 (2020).
- <sup>42</sup> P. Y. Yu, M. Cardona, *Fundamentals of Semiconductors*, Springer, Berlin Heidelberg, 1996.
- <sup>43</sup> S. Kasap, P. Capper (Eds.), *Springer Handbook of Electronic and Photonic Materials*, Springer International, 2017.
- <sup>44</sup> S. Baranovski (Ed.), *Charge Transport in Disordered Solids with Applications in Electronics*, Wiley, USA, 2006.
- <sup>45</sup> A. S. Alexandrov, J. T. Devreese, *Advances in Polaron Physics*, Springer-Verlag Berlin Heidelberg, 2010.
- <sup>46</sup> N. F. Mott, E.A. Davis, *Electronic Processes in Non-Crystalline Materials*, Oxford University Press, Oxford, New York, 2012.
- <sup>47</sup> A. K. Jonscher, *Universal Relaxation Law*, Chelsea Dielectrics Press, London, 1995.
- <sup>48</sup> N. Tsuda, K. Nasu, A. Fujimori, A. Yanase, K. Siratori, *Electronic Conduction in Oxides*, Springer Science Business Media, 2000.
- <sup>49</sup> M. A. Lambert, P. Mark, *Current Injection in Solids*, Academic, New York, 1970.
- <sup>50</sup> S. M. Sze, *Physics of Semiconductor Devices*, Wiley, New York, 1969.
- <sup>51</sup> A. Ghosh, Phys. Rev. B **41**, 1479 (1990).
- <sup>52</sup> M. L. Crespillo, J. T. Graham, F. Agulló-López, Y. Zhang, W. J. Weber, Crystals **9**, 95 (2019).
- <sup>53</sup> X. Hao, Z. Wang, M. Schmid, U. Diebold, C. Franchini, Phys. Rev. B **91**, 085204 (2015).
- <sup>54</sup> B. Wang, P. Saadatkia, F.A. Selim, D. Look, J. Electron. Mater. **47**, 604 (2018).